Oncogene (2012), 1–7

www.nature.com/onc

SHORT COMMUNICATION

Profiling phospho-signaling networks in breast cancer using reverse-phase protein arrays

TS Gujral[1,2], RL Karp[1], A Finski[1,3], M Chan[1], PE Schwartz[4], G MacBeath[1,2] and P Sorger[1]

Measuring the states of cell signaling pathways in tumor samples promises to advance the understanding of oncogenesis and identify response biomarkers. Here, we describe the use of Reverse Phase Protein Arrays (RPPAs or RPLAs) to profile signaling proteins in 56 breast cancers and matched normal tissue. In RPPAs, hundreds to thousands of lysates are arrayed in dense regular grids and each grid is probed with a different antibody (100 in the current work, of which 71 yielded strong signals with breast tissue). Although RPPA technology is quite widely used, measuring changes in phosphorylation reflective of protein activation remains challenging. Using repeat deposition and well-validated antibodies, we show that diverse patterns of phosphorylation can be monitored in tumor samples and changes mapped onto signaling networks in a coherent fashion. The patterns are consistent with biomarker-based classification of breast cancers and known mechanisms of oncogenesis. We explore in detail one tumor-associated pattern that involves changes in the abundance of the Axl receptor tyrosine kinase (RTK) and phosphorylation of the cMet RTK. Both cMet and Axl have been implicated in breast cancer, or in resistance to anticancer drugs, but the two RTKs are not known to be linked functionally. Protein depletion and overexpression studies in a 'triple-negative' breast cell line reveal cross talk between Axl and cMet involving Axl-mediated modification of cMet, a requirement for cMet in efficient and timely signal transduction by the Axl ligand Gas6 and the potential for the two receptors to interact physically. These findings have potential therapeutic implications, as they imply that bi-specific receptor inhibitors (for example, ATP-competitive small-kinase inhibitors such as GSK1363089, BMS-777607 or MP470) may be more efficacious than the mono-specific therapeutic antibodies currently in development (for example, Onartuzumab).

Oncogene advance online publication, 3 September 2012; doi:10.1038/onc.2012.378

Keywords: reverse-phase protein arrays; breast cancer; tumor lysate; cell signaling; MET; AXL

Oncogenic selection functions at the level of networks and pathways rather than individual genes.[1] To date, most multiplex analyses of clinical specimens have involved genomic data because measurement of gene sequences and expression levels is reliable and relatively simple. However, expression profiling does not report directly on regulation at the level of protein abundance or post-translational modification, both of which are required to understand the activities of signaling pathways.[2] Protein state can be assayed using conventional immunoblotting, but this technique has relatively low throughput. The throughput of mass spectrometry (LC/MS) is much greater in terms of total number of data-points but relatively large samples are required, a problem when working with clinical specimens, and assaying many samples remains slow. In the past few years, 'Reverse-phase' protein microarrays (RPPAs) have emerged as a way to perform high-throughput immune-based assays on small amounts of material. In an RPPA, thousands of lysates are arrayed in a dense, regular grid onto glass-supported nitrocellulose pads mounted on a microscope slide, which is then probed with a different antibody.[3–8] Subsequent visualization of the bound antibody on each spot provides a quantitative measure of specific antigens in immobilized samples. A drawback of this approach is that only a small subset of antibodies are sufficiently selective to work in an RPPA format[9] largely, because off-target binding by antibodies contributes to the overall signal. Nonetheless, several studies have shown that RPPA technology is effective in mapping intracellular signaling networks in cell lines.[3,10–13] Here, we ask whether RPPAs can also be used to analyze phosphorylation-mediated signal transduction in human tumor samples.

The current study is a collaboration between a company specializing in rapid processing of surgical tissues and an academic group experienced in RPPA analysis (samples of the lysates analyzed in this paper are available from www.proteinbiotechnologies.com for those who wish to follow up our experiments). Analyzing post-translational modifications in clinical samples require that biopsies be processed rapidly to minimize degradation and dephosphorylation: tissue ischemia alters the expression of 10–15% of all genes within 15 min of resection, and ~30% of all proteins change in abundance within 30 min.[14] To minimize the changes in protein abundance and phosphorylation, tumors were flash-frozen in liquid nitrogen within 5–10 min of resection. Adjacent normal tissue was also collected and processed in parallel. Frozen tissue was minced and homogenized in cold modified RIPA buffer and total protein levels were quantified (Bio-Rad Laboratories). Tumors included the major histotypes and stages of breast cancer: most cases ($n = 48$) were classified as ductal carcinoma of varying grade; mucinous and intraductal cancers were represented by three samples each;

[1]Department of Systems Biology, Harvard Medical School, Boston, MA, USA; [2]Department of Chemistry and Chemical Biology, Harvard University, Cambridge, MA, USA; [3]Department of Molecular and Cellular Biology, Harvard University, Cambridge, MA, USA and [4]Protein Biotechnologies Inc., Ramona, CA, USA. Correspondence: Dr G MacBeath or Professor P Sorger, Department of Systems Biology, Harvard Medical School, WAB 438, 200 Longwood Avenue, Boston, MA 02115, USA.
E-mail: gavin_macbeath@hms.harvard.edu or peter_sorger@hms.harvard.edu
Received 23 March 2012; revised 26 June 2012; accepted 13 July 2012

and lobular and a metaplastic tumors by one sample (Supplementary Table S1).

Approximately 100 arrays were printed from normal and tumor-derived extracts (~10 μg total protein per extract), with each array receiving eight depositions per spot to increase the signal-to-noise ratio. Arrays were adhered to bottomless microtiter plates, allowing rapid processing of 100 arrays with 100 different primary antibodies (Figure 1a). Slides were incubated with dye-labeled secondary antibodies and scanned to quantify fluorescence levels on a spot-by-spot basis. Primary antibodies were directed against proteins, or phosphorylated forms of proteins, known to have a role in oncogenic signal transduction. Several thousand antibodies have been screened by us and by others[8,9] to identify the ~5% of commercial antibodies that exhibit sufficient specificity in multiple cell lines (Figure 1b), particularly for the phosphorylated forms of receptor tyrosine kinases (RTKs), and the cytosolic and nuclear proteins they regulate (Figure 1c). To validate, antibodies are screened against a variety of 'biological contexts' using lysate microarrays. Each context represents a specific combination of cellular type and treatment conditions. Based on the statistical significance of the resulting measurements, promising antibody–context pairs are further evaluated by quantitative western blotting. If the two data sets agree ($R^2 \geqslant 0.7$), the then antibody is considered 'validated' for use. Using this strategy, we screened

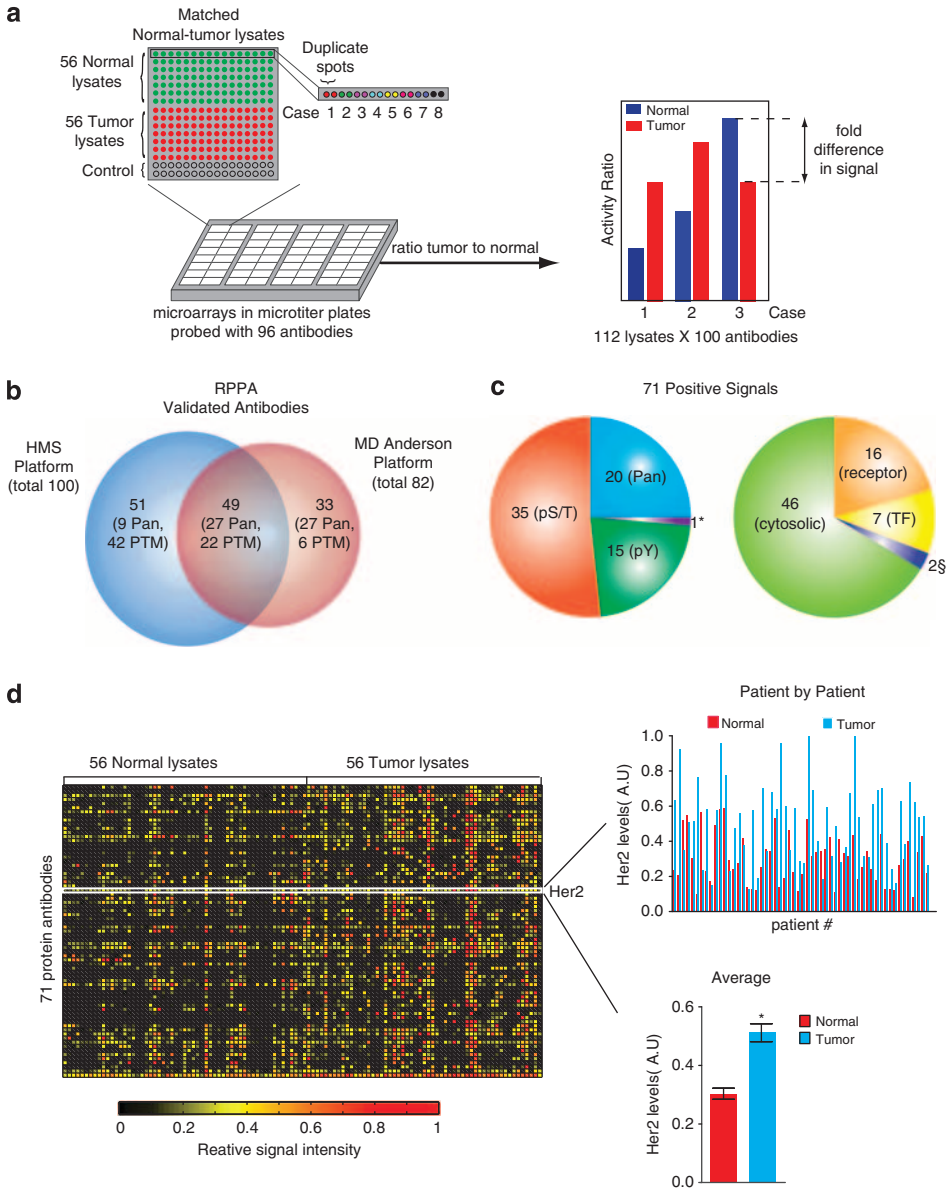

Figure 1. Studying signal transduction in clinical samples by RPPA analysis in patient-matched normal and tumor lysates from 56 cases of breast cancer. (**a**) Schematic of the RPPA screen. Lysates from 56 tumor and corresponding normal samples were arrayed onto nitrocellulose pads, assembled into microtiter plates, and probed with a collection of 100 primary antibodies. A 'fold-difference' in protein measurements was calculated by dividing the activity ratio of a tumor sample by the activity ratio of its matched normal sample. (**b**) Venn diagram of antibodies validated for RPPAs at HMS and MD Anderson.[8,9] (**c**) Breakdown of the 71 antibodies yielding positive signals for breast cancer samples by target and localization. Seventy percent of all antibodies (50/71) were phospho-specific, recognizing modifications that are known to be involved in protein activation. * denotes 'caspase cleavage'; § denotes 'other'subcellular localization. (**d**) A heatmap of 'activity ratios' of 71 protein measurements in 56 normal and corresponding tumor samples. The protein level distribution of HER2/neu across normal (red) and tumor (blue) samples is also highlighted. Lower bar graph showing an average relative intensity of HER2/neu in all cases of normal and tumor samples. Error bars represent s.e.m. * denotes $P < 0.05$.

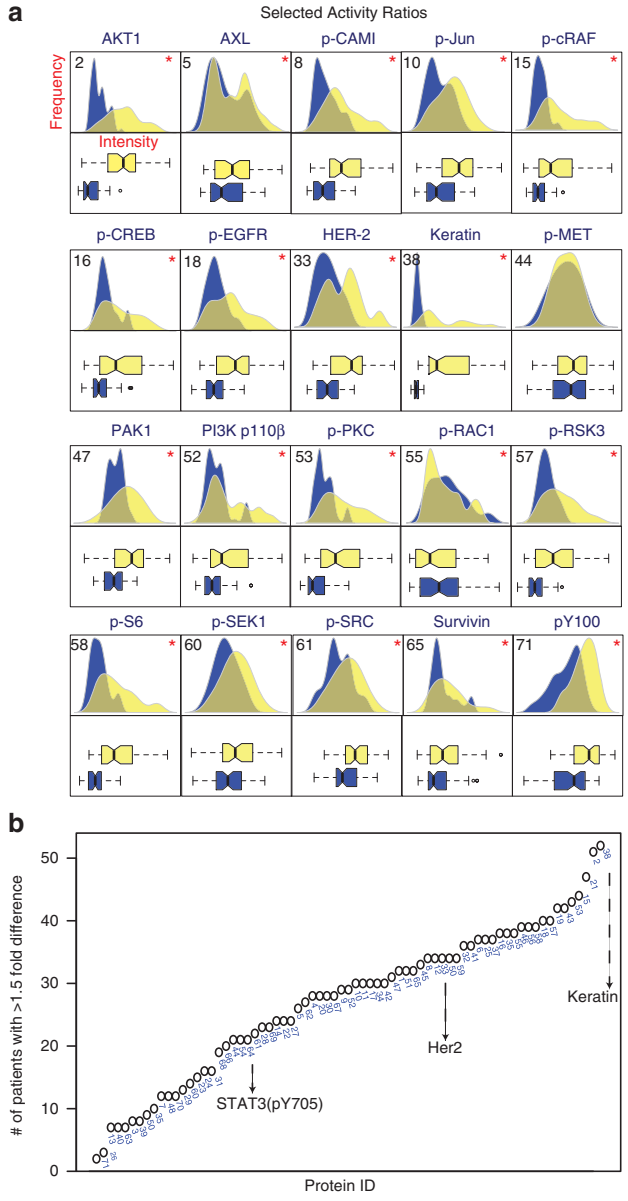

Figure 2. Proteomic measurement for 71 signaling proteins in 56 normal and breast tumor lysates. (**a**) Violin and box plots of probability distributions for a subset of protein measurements. *denotes $P<0.05$ in Kolmogorov–Smirnov test. Blue color denotes normal and yellow color denotes tumor distribution. (**b**) Activity ratios for all 71 protein measurements ranked by the frequency of a 1.5-fold difference across the 56 matched patient samples. Numbers denoted Protein ID for each measurement; see Supplementary Materials for the ID code.

over 400 commercial antibodies and successfully validated 100 of them in one or more biological context.[15,16] Our RPPA antibody panel overlaps, but is not identical to, panels developed by investigators at MD Anderson Cancer Center, who are active in the Cancer Genome Atlas project[8,9] (Figure 1b). With breast cancer samples, 71 members our 100-antibody panel yielded signals above background and were used in the current work to generate a set of ~8,000 intensity measurements, each of which was performed in duplicate (Figure 1c,d). We estimate the technical error in the measurements to be ~ ± 5% (see Supplementary Materials for details). Normalizing the activity of specific measurements to total protein or to a panel of housekeeping proteins has been proven to be effective approaches and we applied the former.[17–19] The activities of phospho-antibodies ;were normalized either to total-protein levels or pan-specific antibodies against the same protein (for example, phospho- and total-FGFR receptor) when the reagents were available. RPPA data were standardized by dividing intensity values for each set of duplicate spots by the maximum intensity value for that particular antibody across all normal and cancer samples, thereby generating a set of 'activity ratios.' In general, distributions of activity ratios were narrower for normal tissue than for tumor tissue (Figure 2a). For measurements such as the total levels of the Her2/ErbB2 receptor (antibody ID 33), the distribution was unimodal for normal tissue and multimodal for tumor tissue (Figure 2a). 'Fold-difference' is a robust metric for scoring the abundance or activities of signaling proteins,[20,21] and we therefore calculated fold-change data by dividing activity ratios for tumor samples by ratios for matched normal tissue on an antibody-by-antibody basis. When data were ranked by the frequency of >1.5-fold difference, we observed significant changes between matched normal and tumor tissue for 54 out of 71 protein signals ($P<0.05$, Kolmogorov–Smirnov test (KS test); Figure 2b). For example, keratin (protein ID:38) was overexpressed in tumor tissue in 55/56 patients (98%), whereas TCF1 (protein ID:20) was overexpressed in 20/56 patients (36%) (see Supplementary Table S2 for ID assignments). Protein biomarkers used to classify breast cancers clinically were elevated to a similar extent in RPPA data and in breast cancers in general: HER2/neu2 levels (which are predictive of responsiveness to trastuzumab[22] were elevated in 24/56 samples (43%) as compared with ~30% of patients, based on the literature.[23] Similarly, estrogen or progesterone receptor levels, which are predictive of responsiveness to anti-hormonal therapy, were elevated in 22/56 (40%) of samples compared with ~60% of patients.[24] Twelve out of fifty-six (21%) samples appeared to derive from triple-negative tumors, as compared with ~20% of patients overall. Thus, RPPA data captures significant variation between tumor and normal tissue, and among different tumors, consistent with current understanding of breast cancer as a complex disease involving multiple subtypes.

As a first step in uncovering patterns of protein co-regulation, we performed unsupervised hierarchical clustering[25] and then drew a threshold in the dendrogram to highlight 12 clusters (that is, with an average cluster size of six specimens; Figure 3a). Diagnostic biomarkers were observed to fall into distinct groups: HER2/neu co-clustered in group II with pro-survival signaling molecules such as pAkt1, pPI3K, pRSK3, pGSK3β, PDGFRβ and insulin receptor; progesterone receptor co-clustered in group X with Vav1, peIF4G, pPLA2; and ER clustered by itself (group XI). It has been shown that mapping clusters of co-expressed genes onto pathways increases information content and intepretability.[26–30] We therefore mapped RPPA clusters onto pathways derived from Gene Network Central Pro (GNCPro); an online resource of literature-curated interaction graphs derived from protein–protein interaction and gene co-expression data.[31] In general, co-clustering RPPA measurements mapped onto known RTK signaling networks. For example, the cluster containing phosphorylated EGF receptor (pY845, group I) also contained the phosphorylated forms of kinases known to function downstream of epidermal growth factor receptor (EGFR) such as Raf1-pS289/296/301, S6K-pS235/236, CAM1-pS81 and PKC-pS660 (Figure 3b). Phosphorylated forms of ERK (pT202/pY204), MEK (pS217/pS221) and S6K (pS240/pS244) kinases made up group VIII, consistent with the known topology of the MAPK signaling cascade and its importance in breast cancer[32] (Supplementary Figure S1).

We focused follow-up analysis on the cluster containing the RTK cMet (whose ligand is hepatocyte growth factor (HGF)): cMet levels are not currently used as a prognostic biomarker in breast cancer patients, but overexpression of the receptor is associated with poor clinical outcome, independent of HER2/neu status,[33] and several drugs targeting cMet are currently in clinical

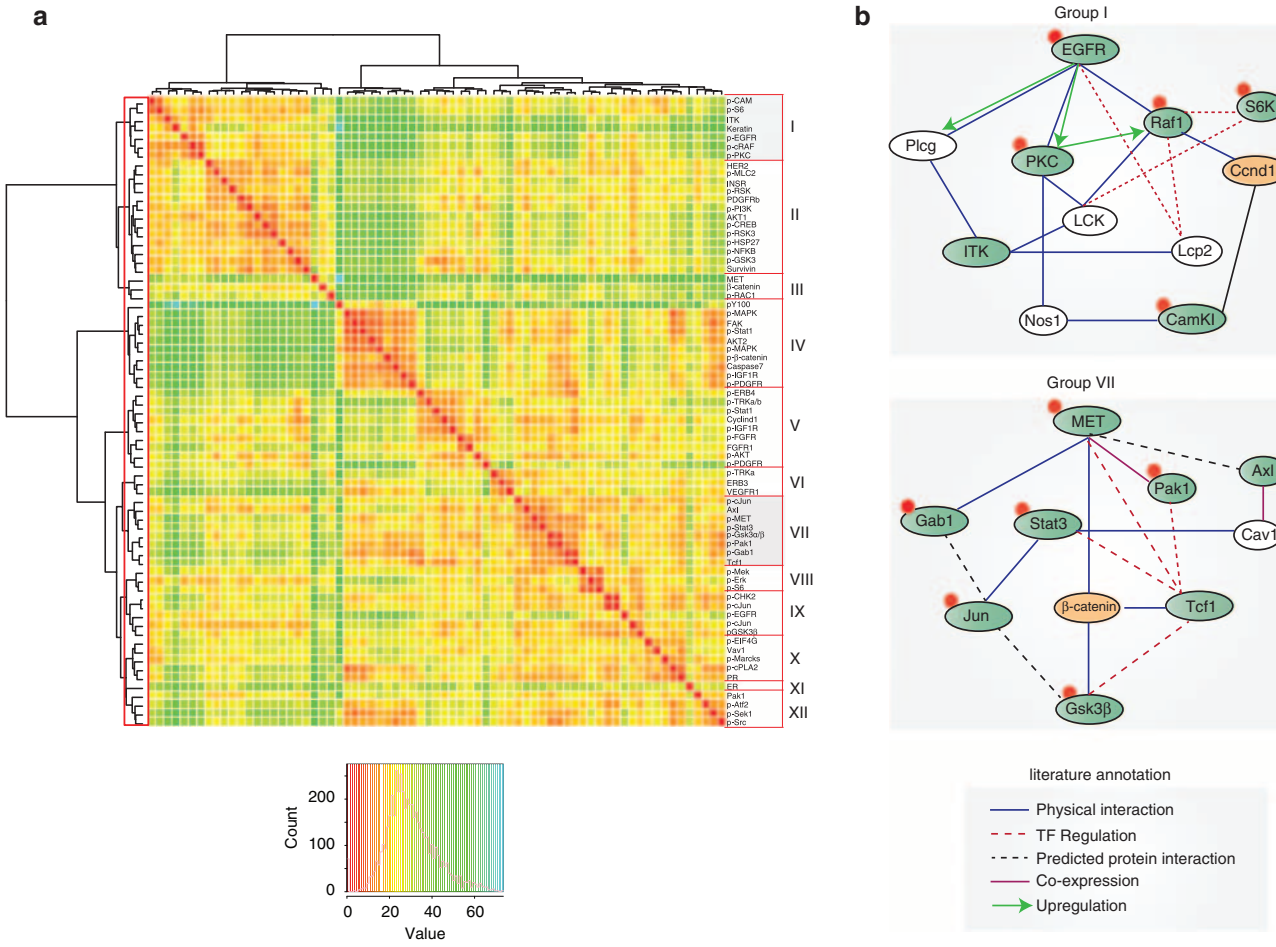

Figure 3. Proteomic profiling of clinical breast cancer specimens reveals distinct network topologies. (**a**) Unsupervised cluster map showing correlation between 71 protein measurements. The map is graded to generate 12 distinct clusters (labeled I–XII), based on activity ratios across all samples. The clusters containing EGFR (Cluster I) and cMet (Cluster VII) are highlighted. (**b**) Protein-interaction networks of clusters containing EGFR and cMet. Protein-interaction networks were constructed for each of these clusters using the GNCPro tool. The proteins measured in this study that clustered together are highlighted in green. Red circle denotes phosphorylation measurement. First neighbors of selected proteins are shown in white. Proteins that were measured but do not fall within the cluster are highlighted in orange. Three receptor tyrosine kinases involved in breast cancer, EGFR, Her2 and cMet, form three distinct clusters. The EGFR network cluster (cluster I) includes pPLCγ, pPKC, ITK, pRAF, pS6 and pCAMI kinases. The data show that the phosphorylation of cMet kinase correlated with phosphorylation of its downstream substrates, Gab1 and Stat3, consistent with established network topology of cMet signaling (cluster VII).[52–55] Phosphorylation of cMet also correlated with phosphorylation of c-Jun and protein levels of Tcf1. In addition to these known components of cMet pathway, measurements for the phosphorylation p21-activated kinase (Pak1) and total levels of Axl fell in the same cluster.

development.[34] We observed that levels of active cMet-pY1349 (group VII) clustered away from total HER2, ER and PR, and from pEGFR (pY845, and pY1173), but correlated well with the total level of the Axl receptor ($R^2 = 0.870$, $P < 0.0001$) and the phosphorylated form of the Stat3 transcription factor ($R^2 = 0.883$, $P < 0.0001$), generating a well-connected GNCPro network that also contained the phospho forms of the Gab1 adapter (pY627), kinases such as Pak1 (pS199/pS204) and GSK3β (pS21/pS9) and the transcription factor cJun (pT91/pT93). Total levels of Tcf1 also fell in this group. Axl is a member of the TAM (Tyro-Axl-Mer) family of receptor tyrosine kinases and has previously been shown to have a role in the motility and invasiveness of breast cancer cells.[35,36] Large-scale network reconstruction suggests an interaction between cMet and Axl[37,38] and the two receptors are co-regulated by miR-34a in breast cancer cell lines.[39]

As a statistically rigorous way to investigate possible co-regulation of Axl and cMet in RPPA data, we turned to structured Bayesian inference involving 11 assays for proteins known to be involved in cMet and Axl signal transduction (10 phospho-proteins and 1 total protein, most of which clustered in group 7). We considered 15 network topologies, all of which involved the class random variable cancer versus normal. The performance of these models was compared to that of four networks in which the cMet and Axl receptors were presumed to covary with cannonical downstream effectors such as Raf and Akt. To learn the parameters of the Bayesian networks, data on RPPA activity ratios were discretized (Supplementary Text and Figure S2) and inference performed on a training- and test-set. The greatest generalization accuracy (82%) was acheived with a network containing the interactions pcMet → Axl, pcMet → pRaf and pRaf → pAkt; adding more interactions decreased the quality of the inference, showing that simpler networks captured all of the available data. Covariation captured by Bayesian inference is not evident from simple inspection of individual probability distributions for p-cMet and total Axl (Figure 2a): p-cMet levels are unimodal and nearly identical in normal and tumor samples, whereas total Axl levels are bimodally distributed in tumor samples (and have a higher mean value; $P < 0.05$, KS-test; Figure 2b). Bayesian network analysis captures the fact that higher p-cMet levels correlate with higher levels of total Axl and this covariation also correlates with the activation of Raf and Akt (Figure 4a, Supplementary Figure S2).

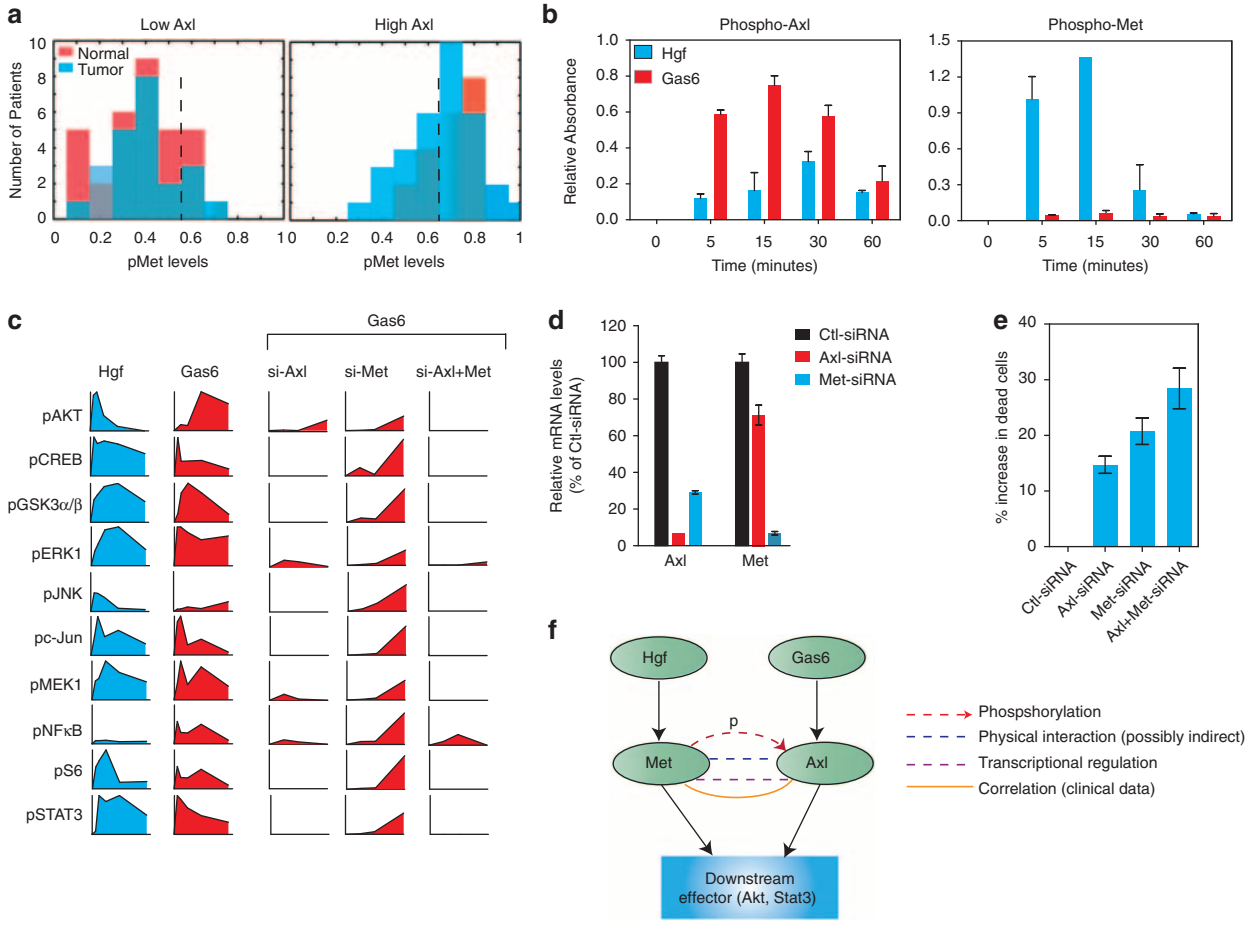

Figure 4. cMet has a role in Gas6-Axl-mediated activation of downstream signaling pathways. (**a**) Frequency distribution of cMet phosphorylation when total Axl levels were low (below the median; left) or high (above the median; right) in both normal and tumor samples. The dashed line denotes the median threshold. (**b**) Bar graphs showing phosphorylation of Axl (left) and cMet (right) upon stimualtion of MDA-MB-231 cells with HGF or Gas6 for the indicated times. Phosphorylation of cMet and Axl receptors were measured using a sandwich ELISA kit (from Cell Signaling Technology). (**c**) Time plots showing phosphorylation of 10 proteins, following the treatment of MDA-MB-231 cells for 0–120 min after treatment with HGF or Gas6 (as inidicated) and assayed using xMAP assays. Time courses to the right show cells treated with siRNA against Axl, cMet or both and exposed to Gas6. (**d**) Bar graph showing relative mRNA levels of Axl and cMet in MDA-MB-231 cells transfected with Axl-siRNA and cMet-siRNA. All values were normalized to control samples transfected with Ctl-siRNA. (**e**) Dual knockdown of Axl and cMet causes increase in cell death, as shown by increase in the number dead cells upon knockdown of Axl, cMet individually or together. Bars represent mean of three independent experiments and error bars represent s.e.m. (**f**) Pathway diagram summarizing proposed mechanisms of cross talk between Axl and cMet kinases, based on this work and the literature. Levels Axl and p-cMet are correlated in breast tumor samples (yellow), and we have shown that treatment of cells with HGF results in Axl phosphorylation (red line); overexpressed Axl and cMet can be co-precipitated (blue line) and the two receptors are transcriptionally co-regulated.[56] The dashes are intended to convey the idea that interactions might be indirect.

To determine if cMet and Axl receptors interact functionally, we turned to breast cancer cell that express both receptors. Exposing MDA-MB-231 triple-negative breast cancer cells to the Axl ligand Gas6 (growth arrest-specific 6) activated multiple downstream signaling cascades, including the PI3K-Akt, MAP kinase, NF-κB and JAK-STAT pathways.[40] Exposing these cells to cMet HGF activated many of the same signaling molecules. To determine if Gas6- and HGF-mediated signaling are inter-dependent at the receptor level, MDA-MB-231 cells were exposed to either Gas6 or HGF, and Axl and cMet receptor phosphorylation assayed by ELISA. We observed that Gas6 caused transient phosphorylation of Axl, peaking at 15 min and falling to baseline levels by 60 min (Figure 4b). No increase in phospho-cMet levels were observed. In contrast, exposure of cells to HGF resulted in transient phosphorylation of both cMet and Axl receptors: p-cMet peaked at 15 min and p-Axl peaked at 30 min (Figure 4b). This suggests cross talk between the two receptors, as has previously been demonstrated for cMet and EGFR in lung tumor cells that have acquired resistance to the EGFR inhibitors gefitinib or between IGF1 recepor and EGFR in breast cancers resistant to erlotinib.[41,42]

To investigate the consequences of Axl and cMet interaction on downstream signaling, we used xMAP micro-sandwich assays[43] to measure the phosphorylation status of 19 signaling proteins at 4–5 time points ranging from 0 to 120 min after exposure of MDA-MB-231 cells to HGF or Gas6 (Figure 4c, Supplementary Figure S3). Both ligands activated Akt (pS473), CREB (pS133), GSK3α/β (pS21/pS9), Erk1 (pT202/pY204), c-Jun (pS63), MEK1 (pS217/pS221), S6 (pT421/pS424) and Stat3 (pS727), but NFκB phosphorylation (pS536) was observed only after Gas6 exposure, as previously described.[44] We then used RNAi to deplete cells of one receptor or the other, and exposed them to Gas6 or HGF. Axl mRNA and protein levels were depleted ~10-fold (Figure 4d, Supplementary Figure S4), and we observed 5–10-fold reductions in Gas6-induced phosphorylation of downstream proteins. Knocking down cMet by RNAi was less efficient (four-fold depletion at the mRNA level and

two-fold at the protein level, Figure 4d, Supplementary Figure S4), resulting in a 2–4-fold reduction and a delay in both HGF and Gas6-mediated phosphorylation of downstream proteins (Figure 4c, Supplementary Figure S3). Knocking down cMet also resulted in a reduction in Axl mRNA levels, consistent with previous reports that the two receptors are co-regulated and consistent with delays in Gas6-mediated phosphorylation of downstream signaling proteins (Figure 4d). The converse was not true, however, Axl depletion did not alter the dynamics or magnitude of HGF-mediated signal transduction. Several studies have shown that knockdown of Met or Axl reduced motility, invasiveness and tumorogenicity in mice.[45–48] In our hands, dual knockdown of Axl and cMet in MDA-MB-231 cells also increased cell death. (Figure 4e) and knockdown of either gene reduced cell migration in a wound-healing assay (Supplementary Figure S5). Thus, both Axl and cMet are involved in typical oncogenic processes in MDA-MB-231 and they may act cooperatively in pro-survival signaling. Co-immunoprecipitation of ectopically expressed Axl and cMet also suggested that the receptors may associate physically: we detected the presence of myc-cMet in HA-Axl immuno-precipitates prepared from lysates of HEK 293 cells overexpressing HA-tagged Axl and myc-tagged cMet (Supplementary Figure S6). Co-purification has been observed in some but not all previously described heterotypic RTK interactions: for example, IGF1R and EGFR, but not cMet and EGFR, co-purify in drug-resistant cell lines.[49] The details of the interaction between cMet and Axl remain to be elucidated and are likely to be complex: although HGF exposure causes both cMet and Axl phosphorylation, knocking down Axl does not appear to alter HGF-mediated phosphorylation of downstream proteins. In contrast, Gas6 exposure results only in Axl phosphorylation, but knocking down cMet alters the timing and magnitude of Gas6-mediated signaling (Figure 4f). Despite these complexities, cell line data support the findings from RPPA analysis showing that Axl and cMet receptors exhibit cross talk and may interact physically in breast cancer cells.

In this paper, we show that RPPA analysis can be used to assay the activation state of signaling proteins in lysates derived from primary tumors. Patterns of protein phosphorylation are remarkably diverse from one tumor to the next, but are consistent with the known topologies of oncogenic signaling pathways and with biomarker-based classification of breast cancer subtypes. The current study benefits from the availability of high-quality lysates, but suffers from a lack of access to genomic data or the clinical histories of the individual patients. We have therefore focused on pathway inference, specifically with regard to the cMet and Axl RTKs. It is highly probable that additional information can be extracted from our RPPA data using more sophisticated analytical methods, and we encourage others to download the data.

If cMet and Axl function coordinately in cancer, as we hypothesize, then it may be advantageous to develop bi-specific antibodies that block both receptors simultaneously. Therapeutic antibodies currently in development that target cMet, such as Onartuzumab are not expected to block Axl, but small molecule cMet kinase inhibitors (GSK1363089, BMS-777607, MP470) do appear to inhibit Axl as well.[34,50,51] More generally, positive results from the current study provide an impetus to clinical investigators, drug companies and institutional review boards to include phosphorylation-rich RPPA analysis in the analysis of clinical data. We note that relatively little work will be required to create a superset of 133 well-validated antibodies spanning both the HMS and MD Anderson RPPA platforms.

CONFLICT OF INTEREST

GM is a Vice President and co-founder, and PKS a co-founder of Merrimack Pharmaceuticals, a biotechnology company that develops anti-cancer drugs. PES is a President and CEO of Protein Biotechnologies, Inc. The remaining authors declare no conflict of interest.

ACKNOWLEDGEMENTS

This study was supported by grants from the National Institutes of Health (R33 CA128726, R21 CA126720, and 5RC1-HG005354) and from the Stand Up to Cancer Project (AACR-SU2C-DT0409). TSG is a Human Frontier Science Program Fellow. RLK is partially supported by NSF 0856285. Supplementary Information accompanies the paper on the Oncogene website.

REFERENCES

1 Vogelstein B, Kinzler KW. Cancer genes and the pathways they control. *Nat Med* 2004; **10**: 789–799.
2 Kolch W, Pitt A. Functional proteomics to dissect tyrosine kinase signalling pathways in cancer. *Nat Rev Cancer* 2010; **10**: 618–629.
3 Sevecka M, MacBeath G. State-based discovery: a multidimensional screen for small-molecule modulators of EGF signaling. *Nat Methods* 2006; **3**: 825–831.
4 Paweletz CP, Charboneau L, Bichsel VE, Simone NL, Chen T, Gillespie JW *et al.* Reverse phase protein microarrays which capture disease progression show activation of pro-survival pathways at the cancer invasion front. *Gene* 2001; **20**: 1981–1989.
5 Tibes R, Qiu YH, Lu Y, Hennessy B, Andreeff M, Mills GB *et al.* Reverse phase protein array: validation of a novel proteomic technology and utility for analysis of primary leukemia specimens and hematopoietic stem cells. *Mol Cancer Ther* 2006; **5**: 2512.
6 Grubb RL, Calvert VS, Wulkuhle JD, Paweletz CP, Linehan WM, Phillips JL *et al.* Signal pathway profiling of prostate cancer using reverse phase protein arrays. *Proteomics* 2003; **3**: 2142–2146.
7 VanMeter A, Signore M, Pierobon M, Espina V, Liotta LA, Petricoin I *et al.* Reverse-phase protein microarrays: application to biomarker discovery and translational medicine. *Expert Rev Mol Diagn* 2007; **7**: 625–633.
8 Hennessy BT, Lu Y, Gonzalez-Angulo AM, Carey MS, Myhre S, Ju Z *et al.* A technical assessment of the utility of reverse phase protein arrays for the study of the functional proteome in non-microdissected human breast cancers. *Clin Proteomics* 2010; **6**: 129–151.
9 Sevecka M, Wolf-Yadlin A, Macbeath G. Lysate microarrays enable high-throughput, quantitative investigations of cellular signaling. *Mol Cell Proteomics* 2011; **10**: M110 005363.
10 Shankavaram UT, Reinhold WC, Nishizuka S, Major S, Morita D, Chary KK *et al.* Transcript and protein expression profiles of the NCI-60 cancer cell panel: an integromic microarray study. *Mol Cancer Ther* 2007; **6**: 820–832.
11 Jiang R, Mircean C, Shmulevich I, Cogdell D, Jia Y, Tabus I *et al.* Pathway alterations during glioma progression revealed by reverse phase protein lysate arrays. *Proteomics* 2006; **6**: 2964–2971.
12 Nishizuka S, Charboneau L, Young L, Major S, Reinhold WC, Waltham M *et al.* Proteomic profiling of the NCI-60 cancer cell lines using new high-density reverse-phase lysate microarrays. *Proc Natl Acad Sci USA* 2003; **100**: 14229–14234.
13 Lin Y, Huang R, Cao X, Wang SM, Shi Q, Huang RP. Detection of multiple cytokines by protein arrays from cell lysate and tissue lysate. *Clin Chem Lab Med* 2003; **41**: 139–145.
14 Spruessel A, Steimann G, Jung M, Lee SA, Carr T, Fentz AK *et al.* Tissue ischemia time affects gene and protein expression patterns within minutes following surgical tumor excision. *Biotechniques* 2004; **36**: 1030–1037.
15 Sevecka M, Wolf-Yadlin A, MacBeath G. Lysate microarrays enable high-throughput, quantitative investigations of cellular signaling. *Mol Cell Proteomics* 2011; **10**: M110 005363.
16 Luckert K, Gujral TS, Chan M, Joos TO, Sorger PK, Macbeath G *et al.* A dual array-based approach to assess the abundance and posttranslational modification state of signaling proteins. *Sci Signal* 2012; **5**: pl1.
17 Gonzalez-Angulo AM, Hennessy BT, Meric-Bernstam F, Sahin A, Liu W, Ju Z *et al.* Functional proteomics can define prognosis and predict pathologic complete response in patients with breast cancer. *Clin Proteomics* 2011; **8**: 11.
18 Carey MS, Agarwal R, Gilks B, Swenerton K, Kalloger S, Santos J *et al.* Functional proteomic analysis of advanced serous ovarian cancer using reverse phase protein array: TGF-beta pathway signaling indicates response to primary chemotherapy. *Clin Cancer Res* 2010; **16**: 2852–2860.
19 Nanjundan M, Byers LA, Carey MS, Siwak DR, Raso MG, Diao L *et al.* Proteomic profiling identifies pathways dysregulated in non-small cell lung cancer and an inverse association of AMPK and adhesion pathways with recurrence. *J Thorac Oncol* 2010; **5**: 1894–1904.
20 Janes KA, Reinhardt HC, Yaffe MB. Cytokine-induced signaling networks prioritize dynamic range over signal strength. *Cell* 2008; **135**: 343–354.
21 Goentoro L, Kirschner MW. Evidence that fold-change, and not absolute level, of beta-catenin dictates Wnt signaling. *Mol Cell* 2009; **36**: 872–884.
22 Burstein HJ, Harris LN, Marcom PK, Lambert-Falls R, Havlin K, Overmoyer B *et al.* Trastuzumab and vinorelbine as first-line therapy for HER2-overexpressing

metastatic breast cancer: multicenter phase II trial with clinical outcomes, analysis of serum tumor markers as predictive factors, and cardiac surveillance algorithm. *J Clin Oncol* 2003; **21**: 2889–2895.
23 Slamon DJ, Clark GM, Wong SG, Levin WJ, Ullrich A, McGuire WL. Human breast cancer: correlation of relapse and survival with amplification of the HER-2/neu oncogene. *Science* 1987; **235**: 177–182.
24 Isola JJ. Immunohistochemical demonstration of androgen receptor in breast cancer and its relationship to other prognostic factors. *J Pathol* 1993; **170**: 31–35.
25 Herrero J, Valencia A, Dopazo J. A hierarchical unsupervised growing neural network for clustering gene expression patterns. *Bioinformatics* 2001; **17**: 126–136.
26 Vaske CJ, Benz SC, Sanborn JZ, Earl D, Szeto C, Zhu J *et al.* Inference of patient-specific pathway activities from multi-dimensional cancer genomics data using PARADIGM. *Bioinformatics* 2010; **26**: i237–i245.
27 Subramanian A, Tamayo P, Mootha VK, Mukherjee S, Ebert BL, Gillette MA *et al.* Gene set enrichment analysis: a knowledge-based approach for interpreting genome-wide expression profiles. *Proc Natl Acad Sci USA* 2005; **102**: 15545–15550.
28 Storey JD, Tibshirani R. Statistical methods for identifying differentially expressed genes in DNA microarrays. *Methods Mol Biol* 2003; **224**: 149–157.
29 Pe'er D, Hacohen N. Principles and strategies for developing network models in cancer. *Cell* 2011; **144**: 864–873.
30 Makretsov NA, Huntsman DG, Nielsen TO, Yorida E, Peacock M, Cheang MCU *et al.* Hierarchical clustering analysis of tissue microarray immunostaining data identifies prognostically significant groups of breast carcinoma. *Clin Cancer Res* 2004; **10**: 6143.
31 Liu G, Fong E, Zeng X. GNCPro: navigate human genes and relationships through net-walking. *Adv Exp Med Biol* 2010 253–259.
32 Menashe I, Maeder D, Garcia-Closas M, Figueroa JD, Bhattacharjee S, Rotunno M *et al.* Pathway analysis of breast cancer genome-wide association study highlights three pathways and one canonical signaling cascade. *Cancer Res* 2010; **70**: 4453.
33 Lengyel E, Prechtel D, Resau JH, Gauger K, Welk A, Lindemann K *et al.* C-Met overexpression in node-positive breast cancer identifies patients with poor clinical outcome independent of Her2/neu. *Int J Cancer* 2005; **113**: 678–682.
34 Underiner TL, Herbertz T, Miknyoczki SJ. Discovery of small molecule c-Met inhibitors: evolution and profiles of clinical candidates. *Anticancer Agents Med Chem* 2010; **10**: 7–27.
35 Zhang YX, Knyazev PG, Cheburkin YV, Sharma K, Knyazev YP, Orfi L *et al.* AXL is a potential target for therapeutic intervention in breast cancer progression. *Cancer Res* 2008; **68**: 1905.
36 Gjerdrum C, Tiron C, Høiby T, Stefansson I, Haugen H, Sandal T *et al.* Axl is an essential epithelial-to-mesenchymal transition-induced regulator of breast cancer metastasis and patient survival. *Proc Natl Acad Sci USA* 2010; **107**: 1124.
37 Bowers PM, Pellegrini M, Thompson MJ, Fierro J, Yeates TO, Eisenberg D. Prolinks: a database of protein functional linkages derived from coevolution. *Genome Biol* 2004; **5**: R35.
38 Marcotte EM, Pellegrini M, Thompson MJ, Yeates TO, Eisenberg D. A combined algorithm for genome-wide prediction of protein function. *Nature* 1999; **402**: 83–86.
39 Mackiewicz M, Huppi K, Pitt JJ, Dorsey TH, Ambs S, Caplen NJ. Identification of the receptor tyrosine kinase AXL in breast cancer as a target for the human miR-34a microRNA. *Breast Cancer Res Treat* 2011; **130**: 663–679.
40 Hafizi S, Dahlback B. Signalling and functional diversity within the Axl subfamily of receptor tyrosine kinases. *Cytokine Growth Factor Rev* 2006; **17**: 295–304.
41 Bean J, Brennan C, Shih JY, Riely G, Viale A, Wang L *et al.* MET amplification occurs with or without T790M mutations in EGFR mutant lung tumors with acquired resistance to gefitinib or erlotinib. *Proc Natl Acad Sci USA* 2007; **104**: 20932–20937.
42 Morgillo F, Woo JK, Kim ES, Hong WK, Lee HY. Heterodimerization of insulin-like growth factor receptor/epidermal growth factor receptor and induction of survivin expression counteract the antitumor action of erlotinib. *Cancer Res* 2006; **66**: 10100–10111.
43 Lim CT, Zhang Y. Bead-based microfluidic immunoassays: the next generation. *Biosens Bioelectron* 2007; **22**: 1197–1204.
44 Demarchi F, Verardo R, Varnum B, Brancolini C, Schneider C. Gas6 anti-apoptotic signaling requires NF-kappa B activation. *J Biol Chem* 2001; **276**: 31738–31744.
45 Previdi S, Abbadessa G, Dalo F, France DS, Broggini M. Breast cancer-derived bone metastasis can be effectively reduced through specific c-MET inhibitor tivantinib (ARQ 197) and shRNA c-MET knockdown. *Mol Cancer Ther* 2012; **11**: 214–223.
46 Vuoriluoto K, Haugen H, Kiviluoto S, Mpindi JP, Nevo J, Gjerdrum C *et al.* Vimentin regulates EMT induction by Slug and oncogenic H-Ras and migration by governing Axl expression in breast cancer. *Oncogene* 2011; **30**: 1436–1448.
47 Holland SJ, Pan A, Franci C, Hu Y, Chang B, Li W *et al.* R428, a selective small molecule inhibitor of Axl kinase, blocks tumor spread and prolongs survival in models of metastatic breast cancer. *Cancer Res* 2010; **70**: 1544–1554.
48 Zhang YX, Knyazev PG, Cheburkin YV, Sharma K, Knyazev YP, Orfi L *et al.* AXL is a potential target for therapeutic intervention in breast cancer progression. *Cancer Res* 2008; **68**: 1905–1915.
49 Nahta R, Yuan LX, Zhang B, Kobayashi R, Esteva FJ. Insulin-like growth factor-I receptor/human epidermal growth factor receptor 2 heterodimerization contributes to trastuzumab resistance of breast cancer cells. *Cancer Res* 2005; **65**: 11118–11128.
50 Kataoka Y, Mukohara T, Tomioka H, Funakoshi Y, Kiyota N, Fujiwara Y *et al.* Foretinib (GSK1363089), a multi-kinase inhibitor of MET and VEGFRs, inhibits growth of gastric cancer cell lines by blocking inter-receptor tyrosine kinase networks. *Invest New Drugs* 2012; **30**: 1352–1360.
51 Mahadevan D, Cooke L, Riley C, Swart R, Simons B, Della Croce K *et al.* A novel tyrosine kinase switch is a mechanism of imatinib resistance in gastrointestinal stromal tumors. *Oncogene* 2007; **26**: 3909–3919.
52 Birchmeier C, Birchmeier W, Gherardi E, Woude GFV. Met, metastasis, motility and more. *Nat Rev Mol Cell Biol* 2003; **4**: 915–925.
53 Mood K, Saucier C, Bong YS, Lee HS, Park M, Daar IO. Gab1 is required for cell cycle transition, cell proliferation, and transformation induced by an oncogenic met receptor. *Mol Biol Cell* 2006; **17**: 3717.
54 Sam MR, Elliott BE, Mueller CR. A novel activating role of SRC and STAT3 on HGF transcription in human breast cancer cells. *Mol Cancer* 2007; **6**: 69.
55 Wojcik E, Sharifpoor S, Miller N, Wright T, Watering R, Tremblay E *et al.* A novel activating function of c-Src and Stat3 on HGF transcription in mammary carcinoma cells. *Oncogene* 2006; **25**: 2773–2784.
56 Yeh CY, Shin SM, Yeh HH, Wu TJ, Shin JW, Chang TY *et al.* Transcriptional activation of the Axl and PDGFR-alpha by c-Met through a ras- and Src-independent mechanism in human bladder cancer. *BMC Cancer* 2011; **11**: 139.

Supplementary Information accompanies the paper on the Oncogene website (http://www.nature.com/onc)